CHEMICAL PHYSICS LETTERS

PULSED HEATING OF SURFACES: COMPARISON BETWEEN NUMERICAL SIMULATION, ANALYTICAL MODELS, AND EXPERIMENTS

Jean-Michel PHILIPPOZ, Renato ZENOBI and Richard N. ZARE

Department of Chemistry, Stanford University, Stanford, CA 94305, USA

A general numerical solution and two approximate analytical solutions of the one-dimensional heat diffusion equation are used to calculate the temperature of a surface exposed to pulsed heating. The calculations simulate the case of pulsed CO_2 laser heating of fused quartz. The numerical solution (based on a finite difference model) includes explicitly the temperature dependence of thermal parameters and is in excellent agreement with experimental measurements on the same system. The analytical solutions are unable to reproduce the temperature history of the sample, and their limitations are discussed.

1. Introduction

The temperature evolution of a surface exposed to pulsed heating by a beam of particles (photons, electrons, ions, neutrons) is of major interest in many beam–solid interactions [1] including laser-induced thermal desorption [2], particle-induced sputtering from surfaces [3] and laser ablation [4]. Lasers in particular are increasingly used as a tool for machining materials or in laser surgery [5]. In such practical applications, it is often the temperature evolution which determines the effect of the radiation. We present here a comparison between different approaches to compute the surface temperature history caused by pulsed heating. The calculations simulate the case of fused quartz heated by a pulsed CO_2 laser and are compared to recent measurements on the same system [6]. Although the simulations are carried out for pulsed laser heating, the formalism applies as well to other cases of pulsed heating.

2. One-dimensional heat flow model

The transient temperature profile generated by pulsed heating depends crucially on two parameters: the energy penetration depth $1/\alpha$ and the thermal diffusion length calculated for heat diffusion in a plane during the heating pulse [7] $d=2(Dt)^{1/2}$,

where α (cm^{-1}) is the absorption coefficient, D (cm^2/s) the thermal diffusivity and t (s) the duration of the heating pulse. If the thermal diffusion length is small compared to the beam diameter, the heat flow parallel to the surface can be neglected and the problem may be treated as one-dimensional. The differential equation for the temperature is

$$\frac{\partial T(x,t)}{\partial t} = \frac{\partial}{\partial x}\left(D\frac{\partial T(x,t)}{\partial x}\right) + \frac{E(x,t)}{\rho c_p}, \qquad (1)$$

where E (W/cm^3) is the source term arising from the impinging beam, ρ (g/cm^3) is the sample density and c_p (J/g K) is the sample heat capacity.

Ready [8] has given a solution of this equation for the case of constant thermal parameters and high absorption coefficient (10^5–10^6 cm^{-1})

$$T(x,t) = (1-R)(1/k)(D/\pi)^{1/2}$$

$$\times \int_0^t I(t-\tau)\exp(-x^2/4D\tau)\,\tau^{-1/2}\,d\tau, \qquad (2)$$

where $I(t)$ (W/cm^2) is the incident power density, R is the reflectivity, and k (W/cm K) is the thermal conductivity. The thermal diffusivity is related to the other material parameters by $D=k/\rho c_p$. This equation has been extensively used in calculations of laser heating, with $I(t)$ being the real laser pulse shape [9], a Gaussian profile [10] or a triangular pulse shape

[11,12]; in the latter case, a very convenient analytical expression of the surface temperature rise has been derived by Burgers, Stair and Weitz [12]. A common feature of these solutions is that the laser is treated as a surface heat source. This assumption is valid provided the energy penetration depth is smaller than the thermal diffusion length. In the case of laser heating, this is generally true for metals because of their very large absorption coefficients, but this approximation becomes more questionable for semiconductors and insulators. In addition, the latter often have more strongly temperature-dependent thermal parameters k and c_p.

In such a situation, modeling of the surface temperature can be obtained numerically by writing the heat flow equation in a finite difference formulation. Other possible approaches are using Green's functions [13], integral transforms [14] or calculating effective absorption coefficients and diffusivities [15]. However, such approaches do not always allow the inclusion of temperature-dependent parameters and/or also involve numerical calculations.

3. Finite difference method

In the finite difference method, the solid is considered as a lattice of nodes associated to a volume element. This can be expressed in Cartesian, cylindrical or spherical coordinates depending on the particular geometry of the problem. In the one-dimensional case, the lattice reduces to a single line perpendicular to the surface, and the volume element is a slice of thickness Δx centered around each node. We use here the explicit forward-time difference formulation, but other finite difference techniques are applicable as well [16]. For the internal slices, the energy balance is

$$k \frac{T_{m+1}^p - 2T_m^p + T_{m-1}^p}{\Delta x} \Delta t$$

$$+ I_m^p [1 - \exp(-\alpha \Delta x)] \Delta t$$

$$= \rho c_p \Delta x (T_m^{p+1} - T_m^p) , \qquad (3)$$

where T_m^p is the temperature of the node m at time p, T_m^{p+1} is the temperature at the same position one time interval Δt later, and I_m^p is the heating power incident on slice m. This equation is used to calculate iteratively the temperature of each node:

$$T_m^{p+1} = \frac{D \Delta t}{(\Delta x)^2} (T_{m+1}^p + T_{m-1}^p)$$

$$+ \frac{I_m^p [1 - \exp(-\alpha \Delta x)] \Delta t}{\rho c_p \Delta x}$$

$$+ \left(1 - \frac{2D \Delta t}{(\Delta x)^2}\right) T_m^p . \qquad (4)$$

As the surface itself is a node (the node $m = 0$) the thickness of the first slice is $\frac{1}{2}\Delta x$ and the temperature of the surface is given by

$$T_0^{p+1} = \frac{2D \Delta t}{(\Delta x)^2} T_1^p$$

$$+ \frac{(1-R)I_0^p [1 - \exp(-\frac{1}{2}\alpha \Delta x)] \Delta t}{\frac{1}{2}\rho c_p \Delta x}$$

$$+ \left(1 - \frac{2D \Delta t}{(\Delta x)^2}\right) T_0^p . \qquad (5)$$

The numerical solution is stable if the coefficient of T_m^p is positive [16].

In eqs. (4) and (5), D, ρ, c_p and α can be temperature dependent. If α depends on temperature, then I_m^p must be calculated iteratively by

$$I_m^p = I_{m-1}^p \exp[-\alpha(T_{m-1}^{p-1}) \Delta x] , \qquad (6)$$

with

$$I_1^p = (1-R)I_0^p \exp[-\frac{1}{2}\alpha(T_0^{p-1}) \Delta x] . \qquad (7)$$

These equations can be easily programmed on a personal computer [#1]. By reducing the size of Δx and Δt, the numerical approximation can be made as exact as desired but at the expense of more computer time.

4. Results and discussion

We compare the results of different possible calculations for the particular example of fused quartz heated by a 10 μs CO_2 laser pulse. This is a critical test case for the approximation of the laser as a surface heat source because the optical penetration depth

---

[#1] A program for an IBM PC (and compatible systems) is available from the authors.
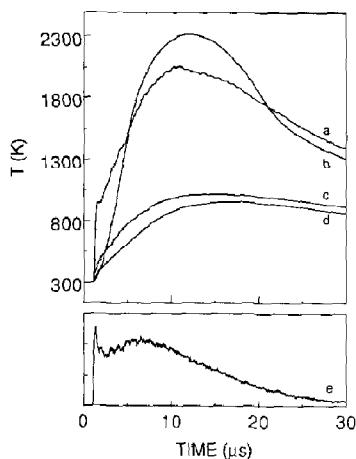
Fig. 1. Surface temperature calculated with (a) eq. (2), (b) with the analytical solution for a triangular pulse [12], using the thermal parameters of fused quartz at their 300 K value. This is compared with the experimental measurement (c) and with the finite difference calculation (d). The same CO_2 laser pulse profile, shown as (e), and incident energy (1.4 J/cm^2) were used in all cases.

is only about 40% smaller than the thermal diffusion length (3.7 μm [2] compared to 5.8 μm [17]). Furthermore, the results can be compared to a recent measurement on the same system obtained by using a calibrated Pt thin film resistance thermometer [6].

The surface temperature calculated with eq. (2) is shown in fig. 1a for the laser pulse profile shown as

[2] The absorption coefficient of the fused quartz sample used in the experiments of ref. [6] was measured by FTIR to be $\alpha \approx 2.7 \times 10^3$ cm^{-1} at 10.6 μm and room temperature, with an uncertainty of $+0.6 \times 10^3 / -0.3 \times 10^3$ cm^{-1}.

fig. 1e. Fig. 1b shows the result of the calculation using the analytical solution [12] based on a triangular approximation to the pulse shape (rise time 4 μs, fall time 16 μs [3]). The maximum temperature rise ΔT_{max} and the time τ_{max} to reach this maximum are summarized in table 1. For these calculations, k, c_p and ρ were assumed to have their values at 300 K. In this case, both the shape of the curves and the value of ΔT_{max} are dramatically different from the measurement with the same pulse profile and incident energy shown in fig. 1c. If instead k and c_p are chosen at 900 K to represent some mean value over the temperature profile (neglecting the variation of ρ), then ΔT_{max} decreases to 1065 K (eq. (2)) or 1222 K (triangular approximation), but the shape of the curves does not change because it is determined by the integral in eq. (2).

These discrepancies demonstrate that our case is beyond the validity domain of both analytical solutions. Although the optical penetration depth is smaller than the thermal diffusion length, these two quantities are still of the same order of magnitude for this case, so that pulsed laser heating cannot be considered to be simply a surface heat source. Furthermore, the temperature dependence of the thermal parameters is important and must be taken into account in the calculation.

[3] Different triangular approximations of this pulse shape conserving the nominal fwhm of 10 μs could be chosen (for example rise time 0.5 μs, fall time 19.5 μs, to give more importance to the early spike). As shown by Burgess et al. [12], the shape of the temperature profile depends on this choice, but the maximum temperature varies by less than 15%.

Table 1

Maximum temperature rise (ΔT_{max}) and time to reach this maximum (τ_{max}) for different calculations. In each case, the laser pulse energy is 1.4 J/cm^2 and the laser temporal profile is as shown in fig. 1e. The corresponding experimental result is also listed

Method	Parameters	ΔT_{max} (K)	τ_{max} (μs)
eq. (2)	$k(300 \text{ K})$, $c_p(300 \text{ K})$	1765	10.0
analytical [12]	$k(300 \text{ K})$, $c_p(300, \text{ K})$	2026	11.1
eq. (2)	$k(900 \text{ K})$, $c_p(900 \text{ K})$	1065	10.0
analytical [12]	$k(900 \text{ K})$, $c_p(900 \text{ K})$	1222	11.1
eqs. (4),(5)	$k(T)$, $c_p(T)$, $\alpha = 10^8$	823	9.3
eqs. (4),(5)	$k(T)$, $c_p(T)$, $\alpha = 2.7 \times 10^3$	665	16.4
eqs. (4),(5)	$k(T)$, $c_p(T)$, $\alpha = 9.5 \times 10^2$ [18]	386	22.0
eqs. (4),(5)	$k(T)$, $c_p(T)$, $\alpha = 210 + 1.2(T - 273 \text{ K})$ [19]	209	27.3
experiment [6]		723	14.7

The temperature variation of k and c_p is readily included in the finite difference technique. The precision of the numerical calculation can be tested by comparing its result with the analytical solution for the triangular pulse shape. By using a quasi-infinite absorption coefficient, we can simulate the case of surface heating. With $\alpha = 10^8$ cm^{-1} and thermal constants at their 300 or 900 K values, we found a difference of less than 2 K over all the temperature profile using $\Delta t = 20$ ns and $\Delta x = 500$ nm.

The surface temperature profile is calculated with these Δx and Δt values, and using temperature-dependent values of k and c_p taken from ref. [17] and the measured absorption coefficient of $\alpha = 2.7 \times 10^3$ cm^{-1}; the result is shown in fig. 1d. Without any adjustable parameter, the overall shape, the maximum temperature, and the high initial heating rate are in good agreement with the measurement [6] (fig. 1c). The remaining discrepancies can be ascribed to uncertainties in the fluence measurement (estimated to be about 15%) and in the absorption coefficient (see below).

Two other experimental results are also well reproduced by the finite difference calculations. First, the shape of the surface temperature profile hardly changes for fluences up to 1.6 J/cm^2: the maximum is always reached after $\tau_{max} = 16.5 \pm 0.5$ µs. Second, the dependence of ΔT_{max} on the fluence is nearly in this range: fig. 2 shows the calculated maximum temperature rise compared to the measured values of ref. [6] and the results of calculated with eq. (2) where k and c_p have their 900 K values. The difference between the finite difference calculation and the experiment is always less than 10%, whereas eq. (2) overestimates the maximum temperature jump by as much as 50%.

We performed some other calculations to determine how sensitive the surface temperature profile is to the parameters of the system. The influence of the absorption coefficient α is of particular interest since different values are found in the literature [18,19]. These differences in the absorption coefficient might be due to impurities causing a shift in one of the very strong absorption band of SiO$_2$ centered at 9.2 and 12.7 µm in crystalline quartz [20]. Consequently, we also measured the absorption coefficient of the fused quartz used in the experiments of ref. [6]. Results are shown for $\alpha = 10^8$ cm^{-1} (quasi-infinite limit, fig. 3a); $\alpha = 2.7 \times 10^3$ cm^{-1} (measured, see footnote 2, fig. 3c); $\alpha = 9.5 \times 10^2$ cm^{-1} (ref. [18], fig. 3d), and $\alpha = 2.1 \times 10^2 + 1.2(T - 273$ K) cm^{-1} (ref. [19], fig. 3e); the measured surface temperature profile is shown again in fig. 3b for comparison. The corresponding values of ΔT_{max} and τ_{max}, which are listed in table 1, vary by
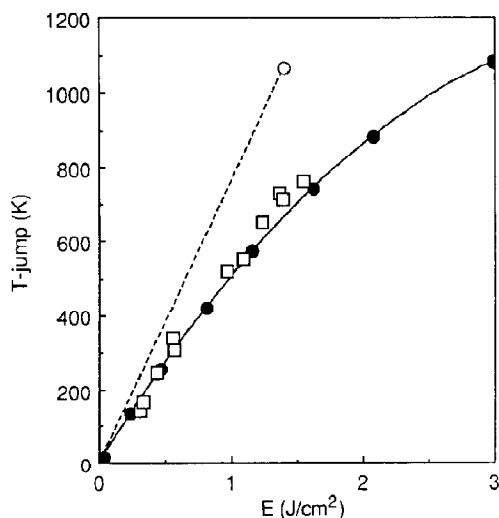

Fig. 2. Maximum temperature rise as function of the incident energy: (●) finite difference calculation, (○) eq. (2) with k and c_p at their 900 K values, (□) measurements from ref. [6].
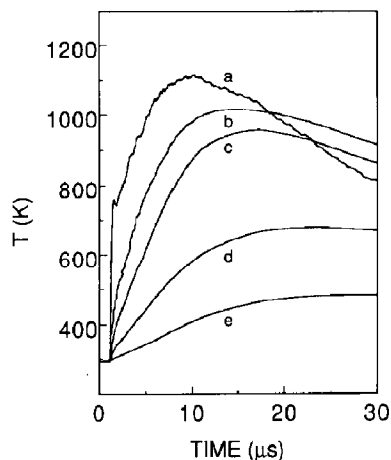

Fig. 3. Surface temperature profiles for different absorption coefficients: (a) $\alpha = 10^8$ cm^{-1} (quasi-infinite limit); (c) $\alpha = 2.7 \times 10^3$ cm^{-1} (measured); (d) $\alpha = 9.5 \times 10^2$ cm^{-1} (ref. [18]); and (e) $\alpha = 2.1 \times 10^2 + 1.2(T - 273$ K) cm^{-1} (ref. [19]). The experimental measurement with the same laser pulse profile is shown as (b).

more than a factor of 3. This comparison demonstrates that the absorption coefficient is a crucial but sometimes poorly determined parameter.

It is also apparent in fig. 3 that the approximation of pulsed laser heating as a surface heating source is not sufficient in this case, even with temperature-dependent thermal parameters. However, we found that the surface temperature profiles calculated with $\alpha = 10^8$ cm^{-1} and $\alpha = 10^5$ cm^{-1} differ by less than 15 K, whereas for $\alpha = 2 \times 10^4$ cm^{-1}, the initial temperature jump corresponding to the early spike in the laser pulse profile is 200 K smaller. This indicates that with a thermal diffusion length of 5.8 μm, the optical penetration depth should be smaller than 0.1 μm for laser irradiation to be considered as a surface heating source.

The other important parameters of the pulsed heated material (k, ρ and c_p) are generally better known and are expected to be less sample dependent than the optical properties. Ref. [17] lists several different determinations of $k(T)$ and $c_p(T)$ for fused quartz, as well as recommended values; in the range 300–1000 K, all determinations, except one, are within 10% of the recommended values. Fig. 4 shows the result of calculations with (a) the lowest value of $k(T)$, (b) the recommended value of $k(T)$, and (c) the highest value of $k(T)$; the other possible combinations of $k(T)$ and $c_p(T)$ give surface tem-
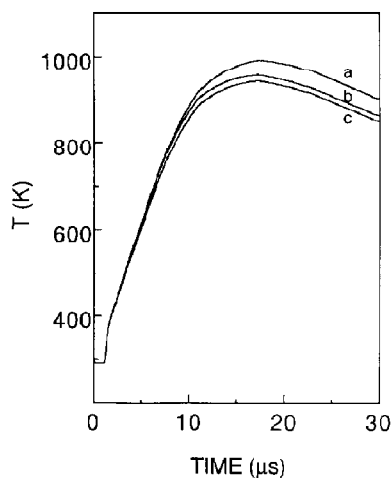

Fig. 4. The surface temperature profiles obtained with different determinations of the thermal conductivity of fused quartz (from ref. [17]) are compared: (a) minimum value of $k(T)$, (b) recommended value of $k(T)$, and (c) maximum value of $k(T)$.

perature profiles intermediate between curves (a) and (c). The small changes associated to these thermal parameter variations can be considered as a "thermal error domain" in the calculation; in our case, it is approximately half the width of the "optical error domain" given by the results of calculations with the extreme values of the uncertainty in α, namely $\alpha = 3.3 \times 10^4$ cm^{-1} and $\alpha = 2.4 \times 10^4$ cm^{-1}.

The thermal parameters of fused quartz, k and c_p, increase nearly linearly with temperature so that the diffusivity is roughly constant from 300 to 800 K (within 10%); at higher temperatures, both are nonlinear and k increases faster than c_p. Calculations show that for laser fluences creating a maximum temperature in the range 300–800 K, the shape of the surface temperature profile hardly changes and the dependence of ΔT_{max} on the incident laser fluence is nearly linear. These two results are valid both for $\alpha = 2.7 \times 10^3$ cm^{-1} and $\alpha = 10^8$ cm^{-1}. The latter tends to indicate that the thermal diffusivity should be constant for using the surface heating model (eq. (2)).

In summary, we have carried out a numerical solution of the one-dimensional heat diffusion equation using a personal computer to simulate accurately the temperature rise induced by a pulsed CO$_2$ laser in fused quartz. Standard analytical models were also evaluated, but failed to reproduce the experimentally determined temperature history. The finite difference numerical method is particularly well suited for cases where the parameters k, c_p or α are strongly temperature dependent, or when the thermal diffusion length is of the same order of magnitude or smaller than the energy penetration depth. Even in cases where the surface heating approximation is acceptable, the inclusion of temperature-dependent thermal parameters may still play an important role in the quantitative computation of heating and cooling rates.

References

[1] Mater. Res. Soc. Symp. Proc. 51 (1986); 100 (1988).

[2] P.C. Stair and E. Weitz, J. Opt. Soc. Am. B 4 (1987) 255;
R.B. Hall and S.J. Bares, Pulsed-laser-induced desorption studies of the kinetics of surface reactions, in: Chemistry and structure at interfaces, eds. R.B. Hall and A.B. Ellis (VCH Publishers, Deerfield Beach, 1986).

[3] A. Benninghoven, A.M. Huber and H.W. Werner, eds., SIMS VI (Wiley, New York, 1987).

[4] B.J. Garrison and R. Srinivasan, J. Appl. Phys. 57 (1985) 2909;
D. Dijkkamp, A.S. Gozdt, T. Venkatesan and X.D. Wu, Phys. Rev. Letters 58 (1987) 2142.

[5] V.S. Lethokov, Nature 316 (1985) 325.

[6] R. Zenobi, J.H. Hahn and R.N. Zare, Chem. Phys. Letters 150 (1988) 361.

[7] W. Jost, Diffusion in solids, liquids, gases (Academic Press, New York, 1952).

[8] J.F. Ready, Effects of high-power laser radiation (Academic Press, New York, 1971).

[9] G.J.Q. van der Peyl, J. Haverkamp and P.G. Kistemaker, Intern. J. Mass Spectrom. 42 (1982) 125;
G. Wedler and H. Ruhman, Surface Sci. 121 (1982) 464;
R.B. Hall and A.M. DeSantolo, Surface Sci. 137 (1984) 421.

[10] J.H. Bechtel, J. Appl. Phys. 46 (1975) 1585;
J.L. Brand and S.M. George, Surface Sci. 167 (1986) 341.

[11] J.P. Cowin, D.J. Auerbach, C. Becker and L. Wharton, Surface Sci. 78 (1978) 545.

[12] D. Burgess Jr., P.C. Stair and E. Weitz, J. Vacuum Sci. Technol. A 4 (1986) 1362.

[13] M. Lax, J. Appl. Phys. 48 (1977) 3919.

[14] A. Maruani, Y.I. Nissim, F. Bonnouvrier and D. Paquet, Mater. Res. Soc. Symp. Proc. 13 (1983) 123.

[15] D.L. Kwong and D. Kim, Mater. Res. Soc. Symp. Proc. 13 (1983) 111.

[16] A.R. Mitchell, The finite difference method in partial differential equations (Wiley, New York, 1980).

[17] Y.S. Touloukian and C.Y. Ho, eds., Thermophysical properties of matter, Vols. 2, 5 (IFI/Plenum, New York, 1970).

[18] E.D. Palik, Handbook of optical constants of solids (Academic Press, New York, 1985).

[19] A.D. McLachlan and F.P. Meyer, Appl. Opt. 26 (1987) 1728.

[20] W.G. Spitzer and D.A. Kleinman, Phys. Rev. 121 (1961) 1324.